

Published in final edited form as:

Lab Chip. 2008 August ; 8(8): 1386–1393. doi:10.1039/b717043b.

Enrichment of putative stem cells from adipose tissue using dielectrophoretic field-flow fractionation

Jody Vykoukal^{†,a}, Daynene M. Vykoukal^{†,a}, Susanne Freyberg^a, Eckhard U. Alt^{a,b}, and Peter R. C. Gascoyne^a

^aUniversity of Texas M.D. Anderson Cancer Center, Department of Molecular Pathology Unit 951, 7435 Fannin Street, Room 2SCR3.3008, Houston, TX, 77054, USA. Fax: +1 713-834-6105; Tel: +1 713-834-6095

^bDepartment of Medicine, Section of Cardiology, Tulane University Health Sciences Center, New Orleans, Louisiana, 70112, USA

Abstract

We have applied the microfluidic cell separation method of dielectrophoretic field-flow fractionation (DEP-FFF) to the enrichment of a putative stem cell population from an enzyme-digested adipose tissue derived cell suspension. A DEP-FFF separator device was constructed using a novel microfluidic-microelectronic hybrid flex-circuit fabrication approach that is scalable and anticipates future low-cost volume manufacturing. We report the separation of a nucleated cell fraction from cell debris and the bulk of the erythrocyte population, with the relatively rare (<2% starting concentration) NG2-positive cell population (pericytes and/or putative progenitor cells) being enriched up to 14-fold. This work demonstrates a potential clinical application for DEP-FFF and further establishes the utility of the method for achieving label-free fractionation of cell subpopulations.

Introduction

The novel exploitation of microscale phenomena in lab-on-a-chip systems offers the promise of new techniques for the manipulation and analysis of biological and biochemical entities. Dielectrophoresis (DEP) and other electrokinetic forces are ideally suited for use in the microfluidic-microelectronic milieu; such forces have been successfully employed to manipulate or separate all manner of analytes in biological microsystems.¹⁻³ Dielectrophoresis is compelling as a method for cell handling: the DEP force acts directly on cells in a suspension and can be used to distinguish cell populations based on differences in cell properties including cell size; membrane morphology, complexity and integrity; cell internal conductivity; relative nuclear volume; and cytoplasmic organization. Differences in cell dielectric properties can be exploited to separate or identify cell subpopulations^{4,5} and to detect diseased, apoptotic, or damaged cells.⁶⁻⁹ The ability to distinguish cells based on intrinsic properties using DEP offers the potential for straightforward implementation and broad utility. Generally-used existing cell separation methods such as fluorescence-activated cell sorting (FACS) or magnetic-activated cell sorting (MACS) employ antibodies or other molecular recognition elements to target cell populations of interest and require *a priori* knowledge of cell-specific markers, synthesis of

specialized probes directed against these markers, and tagging of cell populations to enable separation.

An important cell separation challenge of current interest is the rapid isolation of stem or progenitor cells from autologous donor tissue for regenerative medicine applications.^{10,11} Recent experimental studies and clinical trials indicate that progenitor cells isolated from a range of adult tissues can stimulate angiogenesis in ischemic tissues and may preserve or rescue cardiac and neuronal function following ischemic insult.¹²⁻¹⁸ In acute treatment scenarios, stem cells need to be harvested, processed, and administered promptly and within the context of existing interventional infrastructure. Moreover, for chronic or less acute maladies, stem cell based therapies are expected to enhance or perhaps even supplant many current orthopedic, plastic and general surgery approaches. In these cases, regenerative treatment options are more likely to gain widespread acceptance if progenitor cell harvesting and enrichment can be readily interfaced with existing treatment protocols. There is a particular interest in the use of adipose tissue-derived stem (or stromal) cells (ADSCs or ASCs) because of the relative ease of obtaining subcutaneous fat tissue and the ability of these cells to be differentiated into several cell types.¹⁹⁻²³

Typical stem cell enrichment methods such as MACS, FACS, and panning by plastic adherence are generally laboratory-based and require tissue harvesting and purification to be carried out days or weeks before actual administration of cell therapy. Furthermore, label or cell culture dependent enrichment methods yield tissue preparations that contain modified, activated or otherwise altered cells; for clinical applications, it is highly preferable that isolated cells be unlabeled, and minimally manipulated.²⁴ Although marker-based separation methods have been used to isolate cell populations of interest, there is considerable debate in the stem cell field as to the specific marker profiles that should be targeted. In this study we demonstrate the enrichment of putative stem cells from a mixed population of adipose-derived cells using a dielectrophoretic field-flow fractionation (DEP-FFF) device fabricated using a hybrid microfluidic-microelectronic flex-circuit approach. Our current generation DEP-FFF device is ideally suited for batch-mode separation and recovery of moderate quantities of cells (<10⁶ cells per run).²⁵⁻²⁷ The DEP-FFF device consists of a thin flow channel with microelectrodes patterned along the bottom surface. When energized, the electrodes provide a height-dependent dielectrophoretic force that is perpendicular to the flow axis and applied continuously along the length of the channel—sufficient differences in the density and dielectric characteristics of various cell types cause them to be positioned in different flow-velocity lamina, thereby resulting in differential elution from the separation chamber. The characteristic velocity of cells within the DEP-FFF separator is persistent and the spatial separation achieved is cumulative, analogous to the theoretical plate concept in column chromatography.²⁸ Therefore, a crucial feature of the DEP-FFF device is the length of the flow channel. Simply creating longer versions of the gold-on-glass electrodes utilized in the early generation of DEP-FFF devices poses a serious fabrication challenge. Serpentine channels were explored as an alternative to this approach, but this embodiment limits the flow channel volume and consequently the number of cells that can be loaded in a given run. In this work we utilize a DEP-FFF chamber construction based upon a unique approach to the fabrication of large active area microelectrodes: a continuous interdigitated, gold-on-polyimide electrode created using a reel-based flex-circuit manufacturing process.

Experimental

Cell isolation

In accordance with Tulane University Institutional Review Board (IRB) approval, solid subcutaneous human adipose samples were obtained from discarded tissue excised during elective body contouring procedures. Adipose tissue was manually minced and digested with

Liberase Blendzyme 3 (Roche Diagnostics product 11–814–184–001) at 4 units per gram tissue in phosphate buffered saline (PBS) at 37 °C with shaking for 40 min.^{22,29} The digest mixture was centrifuged at 400 × *g* to remove adipocytes and liquid fat and then the resultant cellular fraction filtered sequentially through 100 μm, 40 μm, and 10 μm filters (Millipore Steriflip SE1M002M8, BD Falcon basket strainer 352340, and Sefar Nitex 03–11/6, respectively). Cells were washed twice by centrifugation in PBS and the erythrocyte quantity reduced by standard density gradient centrifugation (Histopaque-1077, Sigma-Aldrich, St. Louis, MO).

Immunolabeling

Adipose-derived cells were washed in labeling buffer (PBS with 0.5% BSA, 2 mM EDTA) and incubated with one of the following antibody cocktails: FITC-conjugated anti-CD45 monoclonal antibody (Miltenyi Biotec product 130–080–202), rabbit anti-NG2 polyclonal antibody (1 : 200 dilution, Chemicon International, AB5320) and AlexaFluor 488 Goat anti-rabbit secondary IgG (1 : 100 dilution, Invitrogen A11034), or rabbit anti-nestin polyclonal antibody (1 : 200 dilution, Chemicon International, AB5922) and AlexaFluor 488 Goat anti-rabbit secondary IgG. All primary antibodies were either directed against human epitopes or show human species reactivity. Cells were washed with labeling buffer and analyzed by flow cytometry (Partec Cyflow with Flomax analysis software, Münster, Germany). Mock-labeled, isotype, and secondary antibody-only controls were performed in addition to the above reactions to assess the specificity of labeling and to confirm suitable fluorescence over background for antigen-positive cells. Forward scatter (FSC) data was gated to exclude submicron particles and debris yielding 1.8–3.0 × 10⁵ cells (events) per sample. FL1 vs. FSC bivariate scatter plots for samples labeled with fluorescent probes directed against CD45, nestin and NG2 showed well-defined clusters of marker-positive cells distinct from the normal distribution of the unlabeled cell populations. The geometric mean fluorescence intensity for the marker-positive cell populations was 1.4 to 2.1 orders of magnitude (27–115-fold) brighter than the mock-labeled, isotype, or secondary antibody-only control populations.

DEP-FFF theory

For the experiments described here, DEP-FFF was implemented in hyperlayer mode. In this mode, particles are levitated above an electrode array by negative dielectrophoresis. The levitating negative DEP force, F_{DEPz} (which has been shown to fall exponentially with height above the electrode array) and hydrodynamic lift force are balanced against a sedimentation force, F_{grav} to establish particle equilibrium position, h_{eq} within the parabolic flow profile (Fig. 1). Under the moderate flow rate conditions used in these experiments, the equilibrium height, h_{eq} , for a given particle type is expressed by:

$$h_{\text{eq}} = q^{-1} \left(\frac{2(\rho_p - \rho_m)g}{3\epsilon_m p \operatorname{Re}(f_{\text{CM}}) U^2} \right)$$

where where $q^{-1}(h)$ is the inverse function of the height dependency of the vertical DEP force component, $q(h)$; ρ_p and ρ_m are the density of the particle and suspending medium; ϵ_m is the permittivity of the suspending medium; U is applied RMS voltage; p embodies electrode polarization; and $\operatorname{Re}(f_{\text{CM}})$ is the real portion of the complex Clausius–Mossotti factor given by:

$$f_{\text{CM}} = (\epsilon_c^* - \epsilon_m^*) / (\epsilon_c^* + 2\epsilon_m^*), \epsilon^* = \epsilon - j\sigma / (2\pi f)$$

where ε_c is the permittivity of the particle or cell and $j = \sqrt{-1}$. The force balance equation is always single-valued for hyperlayer DEP-FFF, yielding a unique equilibrium position and elution time for all particles of the same type.

DEP-FFF instrumentation

The body of the DEP-FFF flow chamber (Fig. 2) was machined in-house from cell-cast acrylic stock (Acrylite GP, Cyro Industries). The height of the flow channel was defined using a custom-cast PDMS gasket (Silastic S, Dow Corning). The resulting microfluidic channel was 25 mm wide \times 300 mm long \times 375 μm thick. Gold microelectrodes on polyimide substrate (interdigitated 50 μm lines on a 100 μm pitch) were fabricated by a commercial flex-circuit process (3M Microinterconnect Solutions). Fluid flow was controlled by a laboratory syringe pump (KD Scientific; Holliston, MA) and electrodes were energized using a proprietary digital waveform generator and power amplifier board (InGeneron, Incorporated; Houston, TX).

DEP-FFF processing and flow cytometric analysis

Labeled cell mixtures were washed in iso-osmotic dielectrophoresis buffer (9.5% sucrose, 0.3% dextrose, conductivity-adjusted to 30 mS m^{-1} with PBS) and resuspended at a concentration of 2×10^6 cells mL^{-1} . For each run, approximately 1.4×10^6 cells were loaded into the DEP-FFF separation chamber, allowed to settle for 10 min without fluid flow, and then subjected to a fluid flow rate of 1500 $\mu\text{L min}^{-1}$. The frequency of the applied AC electric field was decreased linearly from 200 kHz to 60 kHz over 40 min, followed by a 30 kHz soak ($3 V_{p-p}$). Collected fractions were analyzed by flow cytometry to follow cell elution from the DEP-FFF chamber. FSC was gated as previously described, resulting in 5×10^3 – 1×10^5 cells (events) per fraction depending on the total cell concentration in the particular fraction. Populations of CD45, nestin and NG2 marker-positive cells exhibited geometric mean fluorescence intensity approximately two orders of magnitude over background.

Results and discussion

The work presented here is a first proof of principle demonstration that dielectrophoretic field-flow fractionation (DEP-FFF) can be applied to the rapid, label-free enrichment of progenitor cells from the stromal vascular fraction, a comparatively crude mixture of cell debris, erythrocytes and nucleated cells that results from enzymatic digestion of freshly harvested adipose tissue. The ultimate goal of these cell enrichment studies is the introduction of a practical method for on-demand preparation of autologous, progenitor cell enriched tissue fractions for clinical use. This study was initiated after considering the scarcity of options for purifying stem cells from primary tissues, the limitations of such methods, and the difficulties inherent in porting these laboratory techniques to the clinical setting. Adipose tissue was expressly chosen as a source of progenitor cells because it can be readily harvested *via* a minimally invasive procedure that can be preformed adjunct to a standard surgical intervention. The DEP-FFF separator platform is designed so that it can be run in an automated manner and such that the separator hardware can be single-use and fabricated using relatively low cost, scalable manufacturing methods. A parallel effort is also underway to develop an upstream system for performing adipose tissue harvesting, enzymatic digestion, and filtering with the intention of realizing a fully integrated, closed, and sterile system for preparation of progenitor cell enriched tissue fractions in the clinic.

Translation of lab-on-a-chip technologies from the research laboratory into the clinic or other “real world” setting requires microsystem designs that are amenable to industrial manufacturing methods. Although the principle aim of the study described here was the enrichment of a stem cell population from a mixed cell sample, an additional aim of the project was to explore microfluidic–microelectronic fabrication techniques that anticipate large-scale

manufacture and offer the prospect for reduced next-stage product development times. Accordingly, the DEP-FFF separator device was built primarily from polymeric materials using a multilayer stack-up approach (Fig. 2). Such materials are readily machined or cast using conventional tools and equipment, allowing prototype devices to be built quickly and at a reasonable cost. Furthermore, mature and relatively inexpensive volume manufacturing techniques exist for the processing of polymeric materials and microelectronic flex circuits. Polymer micromolding techniques can replicate nanometer-scale features and current flex circuit design guides specify conductor width and spacing down to 20 μm with finer pitches available at reduced yields. These capabilities are on the order of those required for many lab-on-a-chip applications and merit further exploration.

For most laboratory research applications and clinical experimentation to date, adipose tissue-derived stem cells are isolated from a heterogeneous tissue preparation referred to as the stromal vascular fraction (SVF) based on their adherence to plastic cell culture flasks after 12–48 h. The SVF is obtained by digesting either solid, minced adipose tissue or lipoaspirate with collagenase and then filtering, washing, and centrifuging the cellular fraction to remove mature adipocytes. SVF contains erythrocytes, leukocytes, fibroblasts, and endothelial cells, as well as preadipocytes, pericytes, other progenitor cells, and digest-generated debris.^{19,22} The further separation of SVF by plastic adherence, or panning, results in a culture of cells with fibroblast-like morphology that is considered the *de facto* adipose-derived stem cell population. It is estimated that only one out of every 30 adipose-derived SVF cells (approximately 3%) adheres to plastic.³⁰

Recent findings suggest that mesenchymal stem cells are often associated with the microvasculature in various tissues and may be related to, derived from, share a niche with, or perhaps even be pericytes or pericyte precursors/progenitors. Several groups have demonstrated the ability of cells expressing one or more pericyte or stromal markers (NG2, 3G5, α -smooth muscle actin (α -SMA), PDGF receptor (PDGFR)- α and PDGFR- β , STRO-1, and CD146/MUC18/MCAM) from various adult tissues to differentiate into other cell types, including osteogenic, adipogenic, chondrogenic and myogenic lineages^{22,31-34} and have therefore postulated that this population in the perivascular niche represents a multipotent mesenchymal stem cell-like reserve distributed throughout the body.^{22,31-39} Recent work has led some researchers to conclude that pericytes and ADSCs share a similar phenotype and niche, while others suggest that ADSCs and pericytes are one in the same. Zannettino *et al.* demonstrate that ADSCs expanded from cells selected for positive expression of pericyte marker 3G5 were capable of differentiation into osteoblasts, adipocytes, and chondrocytes *in vitro* and form ectopic bone *in vivo* in NOD/SCID mice, all in a manner similar to those immunoselected for either STRO-1 or CD146. This progenitor cell-like behavior and the authors' finding that human adult stromal cells derived from adipose tissue "exhibit a perivascular-like phenotype" reinforce the concept of a perivascular stem cell niche in adipose tissue.⁴⁰ Traktuev and colleagues take this concept even further, reporting that ADSCs showed coexpression of mesenchymal, pericytic (including NG2, CD140a (PDGFR- α) and CD140b (PDGFR- β), and smooth muscle markers and that the "cells occupied a pericytic position" *in vivo*, leading them to conclude that the "majority of adipose-derived adherent CD34⁺ cells are resident pericytes".⁴¹

Based on this hypothesis, we selected the molecular markers nestin and NG2 chondroitin sulfate proteoglycan (considered to be general stem cell or pericyte markers, respectively) to monitor and compare the elution of these two cell subpopulations from the DEP-FFF chamber and to gauge the level of enrichment of the putative stem cells in each eluted fraction. The use of molecular markers was solely for the purpose of tracking the fate of various cell subpopulations during DEP-FFF separation. Cell transit times and elution profiles were observed to be independent of cell labeling with fluorophore-conjugated antibodies. The

collagenase-digested, filtered adipose tissue preparation (SVF) was divided, and separate aliquots were fluorescently labeled with FITC-conjugated antibodies against NG2, nestin, or the pan-leukocyte marker CD45. Flow cytometric analysis was performed to assess the cellular make-up of the tissue preparation and determine the starting concentration of the various labeled cell types (see Fig. 3). Digest-generated cell debris and erythrocytes could be distinguished from the nucleated cells by their intrinsic forward and side-scatter characteristics.

Labeled cell mixtures were subjected to DEP-FFF processing as described in the *Experimental* section and the eluted fractions were analyzed by flow cytometry to track the elution of the various cell populations from the chamber. The frequency of the applied AC electric field was decreased linearly from 200 kHz to 60 kHz over 40 min, followed by a 30 kHz soak. This particular DEP-FFF electrode energization scheme was chosen following experiments on approximately fifteen adipose tissue digest samples. The rationale for decreasing the frequency during the separation run is as follows. At 200 kHz, intact cells in the SVF experience positive DEP and are retained in a low flow-velocity lamina near the bottom wall of the DEP-FFF separator. Damaged cells and cell debris are not retained and exit the DEP-FFF separator first. As the frequency applied to the DEP-FFF electrode array is decreased, cells in the digest mixture experience differential negative DEP levitation forces. The magnitude of the levitation force acting on a particular cell depends on the cell dielectric properties, which in turn are a function of the cell membrane and cytoplasmic architecture. Different cell types are driven to different flow lamina in the DEP-FFF separator based on the aggregate effect of their density and specific dielectric properties. Cell types that experience a strong levitation force at relatively higher frequencies elute first, while dense cell types that levitate at lower frequencies elute later. More generalized discourse on cell dielectric properties and the physics of DEP-FFF are available elsewhere.^{1,3,25,26} For the study described here, uniform cell loading, fluid flow, and AC electric field conditions were utilized so that the data from separate runs could be overlaid for comparison purposes.

Fig. 4 shows the elution profiles for the NG2-positive, nestin-positive, and CD45-positive cell populations. For simplicity, we have chosen to show the NG2-negative particles from the NG2-labeled run, but the elution profile of this cell population was nearly identical to that observed for the nestin and CD45 runs and can therefore be considered representative. This NG2-negative population predominantly contains damaged cells and debris (early fractions) and erythrocytes (later fractions). As shown in Fig. 4a, the DEP-FFF method separates the nucleated cell fraction from both the digest-generated cell debris and the bulk of the erythrocyte population. This is significant as debris and erythrocytes comprise a substantial portion of the SVF, but offer no regenerative potential. Additionally, since the DEP-FFF separation is not based on biomarkers, damaged or apoptotic cells are not coenriched with healthy cells as they could be in a MACS or FACS enrichment. The inset shown in Fig. 4b reveals nearly identical elution profiles for cells labeled with antibodies against the two independent putative stem cell markers, NG2 and nestin. The elution peak shift observed between these cells of interest and the mature, CD45-positive leukocytes indicates that the respective cell populations possess different dielectric and density properties and exemplifies the dependence of the DEP-FFF method on intrinsic morphology, size, and density differences between cell types.^{1,3,25,26} In addition to separating the cells of interest from the debris and erythrocytes, we were particularly interested in the relative enrichment of the NG2-positive and nestin-positive cells in the eluted fractions after DEP-FFF processing (see Fig. 5). Relatively rare (<2% in the starting mixture) NG2-positive cells were enriched up to 14-fold. Nestin-positive cells, which showed a slightly higher initial fluorescence labeling level of approximately 4%, were enriched up to 5-fold.

This SVF enrichment data must be evaluated with an understanding that the maximum attainable level of enrichment depends on the relative rarity of the cell type of interest in the starting material. Impressive enrichment factors can be attained by MACS or FACS for bone

marrow mesenchymal stem cells because of their scarcity in the starting tissue. Using a standard plastic-adherence CFU-F (colony forming units fibroblast) assay for mesenchymal stem cell count, bone marrow derived MSCs selected by MACS for STRO-1 showed 950-fold enrichment over unfractionated cells³² and those selected by MACS for STRO-1 and then CD146⁺ by FACS (STRO-1^{BRT}/CD146⁺) showed 2×10^3 -fold enrichment over unfractionated cells.³⁷ However, in tissues with a greater relative percentage of putative stem cells, these methods yield concomitantly lower enrichment values. For example, pooled dental pulp samples subjected to MACS selection for STRO-1⁺ or CD146⁺ provided 6-fold and 7-fold enrichment over unfractionated cells, respectively.³⁷ In a recent study, FACS enrichment of adipose-derived stem/stromal cells from SVF by selection for 3G5 yielded approximately 3-fold enrichment in CFU-F over unsorted cells.⁴⁰ For the adipose samples used in our study, NG2⁺ cells accounted for approximately 2–3% of the total cell population, so the maximum theoretical enrichment level achievable for a pure population would be 33- to 50-fold. This stem cell frequency agrees with the reported observation that approximately one out of every 30 adipose-derived SVF cells adheres to plastic.³⁰ The 14-fold enrichment after DEP-FFF processing (yielding 28% NG2⁺ cells in the most enriched elution fraction) may be quite sufficient for some clinical applications and is significant because the tissue processing method is label-free and rapid. In our experience, variability in DEP-FFF-based cell fractionation is principally of a biological nature and not due to intrinsic system or hardware variation.^{3,27,42} Biological variance is manifest in DEP-FFF elution profiles as a shift in elution time and/or peak broadening; however, a standardized protocol for cell processing and DEP-FFF enrichment can attenuate these effects. In the stromal vascular fraction enrichment experiments described here, the erythrocyte peak elution time is used as a standard reference point when comparing different runs from the same patient sample. For these data we observe good run to run coincidence for the various subpopulation peaks for a given patient sample and good agreement in the relative subpopulation elution times between different patient samples.

DEP-FFF provides a distinct advantage over the standard MACS or FACS cell isolation techniques in that labeling of the cells is not a requisite part of the separation procedure. For cells with known marker profiles, labeling can be employed during development of the DEP-FFF separation protocol to optimize run parameters and then subsequently avoided. In the experiments described here, fluorescent antibody labels were used only passively to enable identification of the various cell types in the starting mixture and to facilitate quantitative assessment of the separation progress and efficiency. Such label-free cell-isolation methods are preferred when preparing samples for clinical applications, as regulatory agencies generally specify additional testing and validation studies for cell-based therapeutics that contain labeled, treated or otherwise modified cell preparations. Additionally, DEP-FFF is much more rapid than the isolation of stem cells from a mixture based on their adherence to plastic cultureware.^{19,20} Cells from a collagenase-digested tissue extract are incubated in plastic culture flasks, and the non-adherent erythrocytes, leukocytes, and debris are washed away after 12–48 h to yield what is generally considered to be a stem cell population. Typically, these cells must also then be expanded in culture before use in a basic or preclinical study. In contrast, a DEP-FFF run can be completed in less than 20 min. Previous investigations in our lab and others have established that exposure to electric fields from DEP electrodes akin to those used in these experiments does not alter cell viability.⁴³⁻⁴⁵ In our initial adipose-derived SVF fractionation experiments, eluted cell fractions were collected into tissue culture media, cultured for 12–24 h and assayed for plastic adherence. Cultures of viable cells possessing a fibroblast-like morphology typically associated with adipose-derived mesenchymal stem cell cultures were observed, confirming that cells remain viable following fractionation by DEP-FFF.

Several groups are actively exploring the basic biology and clinical applications of both the stromal vascular fraction that is obtained following enzymatic digestion of adipose tissue, as well as further purified adipose-derived stem/stromal cells. Selected examples of recent

preclinical work include the transplantation of sheets of monolayered ADSCs into infarcted rat myocardium,⁴⁶ intracoronary administration of ADSCs into infarcted pig myocardium,⁴⁷ use of ADSCs for neuroprotective purposes in a rat intracerebral hemorrhage model,¹⁷ injection of ADSCs into a mouse ischemic limb disease model,⁴⁸ use of ADSCs for periodontal tissue regeneration in rats,⁴⁹ and use of ADSCs to regenerate corneal stroma in rabbits.⁵⁰ Other groups are investigating more rapid, direct clinical methods in which adipose tissue is harvested and the progenitor-cell containing raw SVF or lipoaspirate is immediately applied, without further enrichment, for repair or regeneration within a single operative procedure. Examples include the application of freshly isolated SVF mixed with fibrin glue to treat skull defects (mixture estimated to contain 2–3% stem cells),⁵¹ the use of “purified lipoaspirate” to heal irradiation-induced lesions in human breast,⁵² and a cell-assisted lipotransfer (CAL) technique in which freshly isolated SVF is mixed with lipoaspirate for cosmetic breast augmentation.⁵³

The level of enrichment that is required to yield safe and clinically efficacious adipose derived progenitor cell fractions is yet to be determined. However, for clinical applications, it is anticipated that a freshly prepared, *pro re nata* source of autologous progenitor cells would be favored over heterologous, cultured or banked sources. We are currently working to refine and further enhance the applicability of the DEP-FFF method to the enrichment of stem cells from tissue digests. Planned improvements include modification of the sample loading and flow rate to yield shorter processing times, increasing the number of cells that can be sorted in a single run, altering electrical characteristics of the applied AC electric field gradient to shift the CD45-positive peak further from the putative stem cell peak, and incorporation of an integrated means of detecting and characterizing eluted cells to provide real-time feedback about cell purity and yield.

Conclusions

DEP-FFF processing of a filtered, collagenase-digested adipose tissue suspension isolated the nucleated cell fraction from both the digest-generated cell debris and the bulk of the erythrocytes. Independent DEP-FFF runs yielded nearly identical elution profiles for cells labeled with FITC-conjugated antibodies against two putative stem cell markers, NG2 and nestin. Furthermore, the elution peaks for the putative stem cells were shifted from the peak containing the CD45-positive leukocytes. Overall, the relatively rare (<2% in the starting mixture) NG2-positive cells were enriched up to 14-fold. Further efforts will be made to improve the performance of the DEP-FFF method for enriching and harvesting putative stem cells and other rare cell populations from complex cell mixtures.

Acknowledgements

This work was supported in part by the Alliance of Cardiovascular Researchers. The authors would like to thank Kirsten Daemen, Xiaowen Bai, Yasheng Yan, Thomas Anderson, Greg Stone, Ron Stubbers, John Martin, Grace Wu, Michael Coleman, Andrew Altman, and Edward Newsome for their assistance with various aspects of this project.

References

1. Vykoukal, J.; Vykoukal, DM. *Micro and Nano Manipulations for Biomedical Applications*. Yih, TC.; Talpasanu, I., editors. Artech House; Norwood, MA: 2007. p. 197-213.ch. 7
2. Voldman J. *Annu. Rev. Biomed. Eng* 2006;8:425–454. [PubMed: 16834563]
3. Gascoyne PRC, Vykoukal J. *Electrophoresis* 2002;23:1973–1983. [PubMed: 12210248]
4. Yang J, Huang Y, Wang XJ, Wang XB, Becker FF, Gascoyne PRC. *Biophys. J* 1999;76:3307–3314. [PubMed: 10354456]
5. Castellarnau M, Errachid A, Madrid C, Juarez A, Samitier J. *Biophys. J* 2006;91:3937–3945. [PubMed: 16950844]

6. Becker FF, Wang XB, Huang Y, Pethig R, Vykoukal J, Gascoyne PRC. Proc. Natl. Acad. Sci. U. S. A 1995;92:860–864. [PubMed: 7846067]
7. Wang XJ, Becker FF, Gascoyne PRC. Biochim. Biophys. Acta: Biomembranes 2002;1564:412–420.
8. Labeed FH, Coley HM, Hughes MP. Biochim. Biophys. Acta: General Subjects 2006;1760:922–929.
9. Ratanachoo K, Gascoyne PRC, Ruchirawat M. Biochim. Biophys. Acta: Biomembranes 2002;1564:449–458.
10. Mimeault M, Hauke R, Batra SK. Clin. Pharmacol. Ther 2007;82:252–264. [PubMed: 17671448]
11. Mays RW, van't Hof W, Ting AE, Perry R, Deans R. Expert Opin. Biol. Ther 2007;7:173–184. [PubMed: 17250456]
12. Laflamme MA, Murry CE. Nat. Biotechnol 2005;23:845–856. [PubMed: 16003373]
13. Wollert KC, Meyer GP, Lotz J, Ringes-Lichtenberg S, Lippolt P, Breidenbach C, Fichtner S, Korte T, Hornig B, Messinger D, Arseniev L, Hertenstein B, Ganser A, Drexler H. Lancet 2004;364:141–148. [PubMed: 15246726]
14. Schachinger V, Erbs S, Elsasser A, Haberbosch W, Hambrecht R, Holschermann H, Yu J, Corti R, Mathey DG, Hamm CW, Suselbeck T, Assmus B, Tonn T, Dimmeler S, Zeiher AM. N. Engl. J. Med 2006;355:1210–1221. [PubMed: 16990384]
15. Lipinski MJ, Biondi-Zoccai GG, Abbate A, Khianey R, Sheiban I, Bartunek J, Vanderheyden M, Kim HS, Kang HJ, Strauer BE, Vetrovec GW. J. Am. Coll. Cardiol 2007;50:1761–1767. [PubMed: 17964040]
16. Savitz SI, Rosenbaum DM, Dinsmore JH, Wechsler LR, Caplan LR. Ann. Neurol 2002;52:266–275. [PubMed: 12205638]
17. Kim JM, Lee ST, Chu K, Jung KH, Song EC, Kim SJ, Sinn DI, Kim JH, Park DK, Kang KM, Hyung HN, Park HK, Won CH, Kim KH, Kim M, Kun LS, Roh JK. Brain Res 2007;1183:43–50. [PubMed: 17920570]
18. Zietlow R, Lane EL, Dunnett SB, Rosser AE. Cell Tissue Res 2008;331:301–322. [PubMed: 17901985]
19. Gimble JM, Katz AJ, Bunnell BA. Circ. Res 2007;100:1249–1260. [PubMed: 17495232]
20. Schaffler A, Buchler C. Stem Cells 2007;25:818–827. [PubMed: 17420225]
21. Zuk PA, Zhu M, Ashjian P, De Ugarte DA, Huang JI, Mizuno H, Alfonso ZC, Fraser JK, Benhaim P, Hedrick MH. Mol. Biol. Cell 2002;13:4279–4295. [PubMed: 12475952]
22. Zuk PA, Zhu M, Mizuno H, Huang J, Futrell JW, Katz AJ, Benhaim P, Lorenz HP, Hedrick MH. Tissue Eng 2001;7:211–228. [PubMed: 11304456]
23. Fraser JK, Wulur I, Alfonso Z, Hedrick MH. Trends Biotechnol 2006;24:150–154. [PubMed: 16488036]
24. Fink, DW. FDA Review of Investigational Cell-based Therapies: Resource Tools, Framework and Issues. Center for Biologics Evaluation and Research, U.S. Food and Drug Administration; 2006. <http://www.fda.gov/cber/genetherapy/stemcell031406df.htm>
25. Huang Y, Wang XB, Becker FF, Gascoyne PRC. Biophys. J 1997;73:1118–1129. [PubMed: 9251828]
26. Markx GH, Rousselet J, Pethig R. J. Liq. Chromatogr. Relat. Technol 1997;20:2857–2872.
27. Wang XB, Yang J, Huang Y, Vykoukal J, Becker FF, Gascoyne PRC. Anal. Chem 2000;72:832–839. [PubMed: 10701270]
28. Sant HJ, Gale BK. J. Chromatogr., A 2006;1104:282–290. [PubMed: 16368105]
29. Rodbell M. J. Biol. Chem 1964;239:375–380. [PubMed: 14169133]
30. Mitchell JB, McIntosh K, Zvonic S, Garrett S, Floyd ZE, Kloster A, Di Halvorsen Y, Storms RW, Goh B, Kilroy G, Wu X, Gimble JM. Stem Cells 2006;24:376–385. [PubMed: 16322640]
31. Doherty MJ, Ashton BA, Walsh S, Beresford JN, Grant ME, Canfield AE. J. Bone Miner. Res 1998;13:828–838. [PubMed: 9610747]
32. Gronthos S, Zannettino AC, Hay SJ, Shi S, Graves SE, Kortessidis A, Simmons PJ. J. Cell Sci 2003;116:1827–1835. [PubMed: 12665563]
33. Seo BM, Miura M, Gronthos S, Bartold PM, Batouli S, Brahim J, Young M, Robey PG, Wang CY, Shi S. Lancet 2004;364:149–155. [PubMed: 15246727]

34. Dellavalle A, Sampaolesi M, Tonlorenzi R, Tagliafico E, Sacchetti B, Perani L, Innocenzi A, Galvez BG, Messina G, Morosetti R, Li S, Belicchi M, Peretti G, Chamberlain JS, Wright WE, Torrente Y, Ferrari S, Bianco P, Cossu G. *Nat. Cell Biol* 2007;9:255–267. [PubMed: 17293855]
35. Andreeva ER, Pugach IM, Gordon D, Orekhov AN. *Tissue Cell* 1998;30:127–135. [PubMed: 9569686]
36. Bianco P, Riminucci M, Gronthos S, Robey PG. *Stem Cells* 2001;19:180–192. [PubMed: 11359943]
37. Shi S, Gronthos S. *J. Bone Miner. Res* 2003;18:696–704. [PubMed: 12674330]
38. Howson KM, Aplin AC, Gelati M, Alessandri G, Parati EA, Nicosia RF. *Am. J. Physiol.: Cell Physiol* 2005;289:C1396–C1407. [PubMed: 16079185]
39. Landazuri N, Taylor WR. *Am. J. Physiol.: Cell Physiol* 2005;289:C1361–C1362. [PubMed: 16275735]
40. Zannettino AC, Paton S, Arthur A, Khor F, Itescu S, Gimble JM, Gronthos S. *J. Cell Physiol* 2008;214:413–421. [PubMed: 17654479]
41. Traktuev DO, Merfeld-Clauss S, Li J, Kolonin M, Arap W, Pasqualini R, Johnstone BH, March KL. *Circ. Res* 2008;102:77–85. [PubMed: 17967785]
42. Wang XB, Vykoukal J, Becker FF, Gascoyne PRC. *Biophys. J* 1998;74:2689–2701. [PubMed: 9591693]
43. Wang XJ, Yang J, Gascoyne PRC. *Biochim. Biophys. Acta: General Subjects* 1999;1426:53–68.
44. Ho CT, Lin RZ, Chang WY, Chang HY, Liu CH. *Lab Chip* 2006;6:724–734. [PubMed: 16738722]
45. Borgatti M, Bianchi N, Mancini I, Feriotto G, Gambari R. *Int. J. Mol. Med* 2008;21:3–12. [PubMed: 18097610]
46. Miyahara Y, Nagaya N, Kataoka M, Yanagawa B, Tanaka K, Hao H, Ishino K, Ishida H, Shimizu T, Kangawa K, Sano S, Okano T, Kitamura S, Mori H. *Nat. Med* 2006;12:459–465. [PubMed: 16582917]
47. Valina C, Pinkernell K, Song YH, Bai X, Sadat S, Campeau RJ, Le Jemtel TH, Alt E. *Eur. Heart J* 2007;28:2667–2677. [PubMed: 17933755]
48. Nakagami H, Maeda K, Morishita R, Iguchi S, Nishikawa T, Takami Y, Kikuchi Y, Saito Y, Tamai K, Ogihara T, Kaneda Y. *Arterioscler. Thromb. Vasc. Biol* 2005;25:2542–2547. [PubMed: 16224047]
49. Tobita M, Uysal AC, Ogawa R, Hyakusoku H, Mizuno H. *Tissue Eng.* 2007
50. Arnalich-Montiel F, Pastor S, Blazquez-Martinez A, Fernandez-Delgado J, Nistal M, Alio JL, De Miguel MP. *Stem Cells* 2008;26:570–579. [PubMed: 18065394]
51. Lendeckel S, Jodicke A, Christophis P, Heidinger K, Wolff J, Fraser JK, Hedrick MH, Berthold L, Howaldt HP. *J. Craniomaxillofac. Surg* 2004;32:370–373. [PubMed: 15555520]
52. Rigotti G, Marchi A, Galie M, Baroni G, Benati D, Krampera M, Pasini A, Sbarbati A. *Plast. Reconstr. Surg* 2007;119:1409–1422. [PubMed: 17415234]
53. Yoshimura K, Sato K, Aoi N, Kurita M, Hirohi T, Harii K. *Aesthetic Plast. Surg* 2008;32:48–55. [PubMed: 17763894]

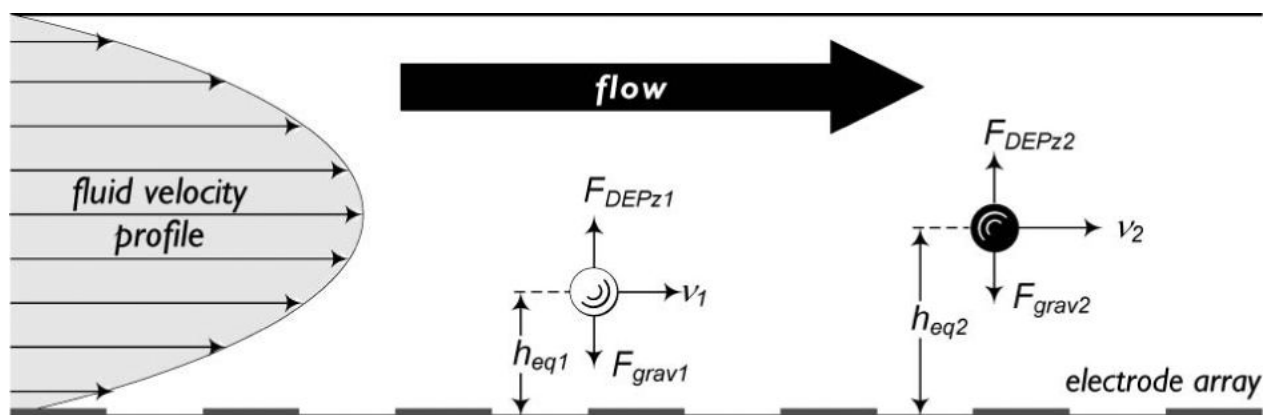


Fig. 1. Principle of dielectrophoretic field-flow fractionation. Particle velocity, v is determined by particle equilibrium height, h_{eq} within the laminar parabolic flow profile. At h_{eq} , the levitating DEP levitation force, F_{DEPz} and sedimentation force, F_{grav} are balanced such that

$$-\frac{4}{3}\pi r^3(\rho_p - \rho_m)g + F_{DEPz} = 0.$$

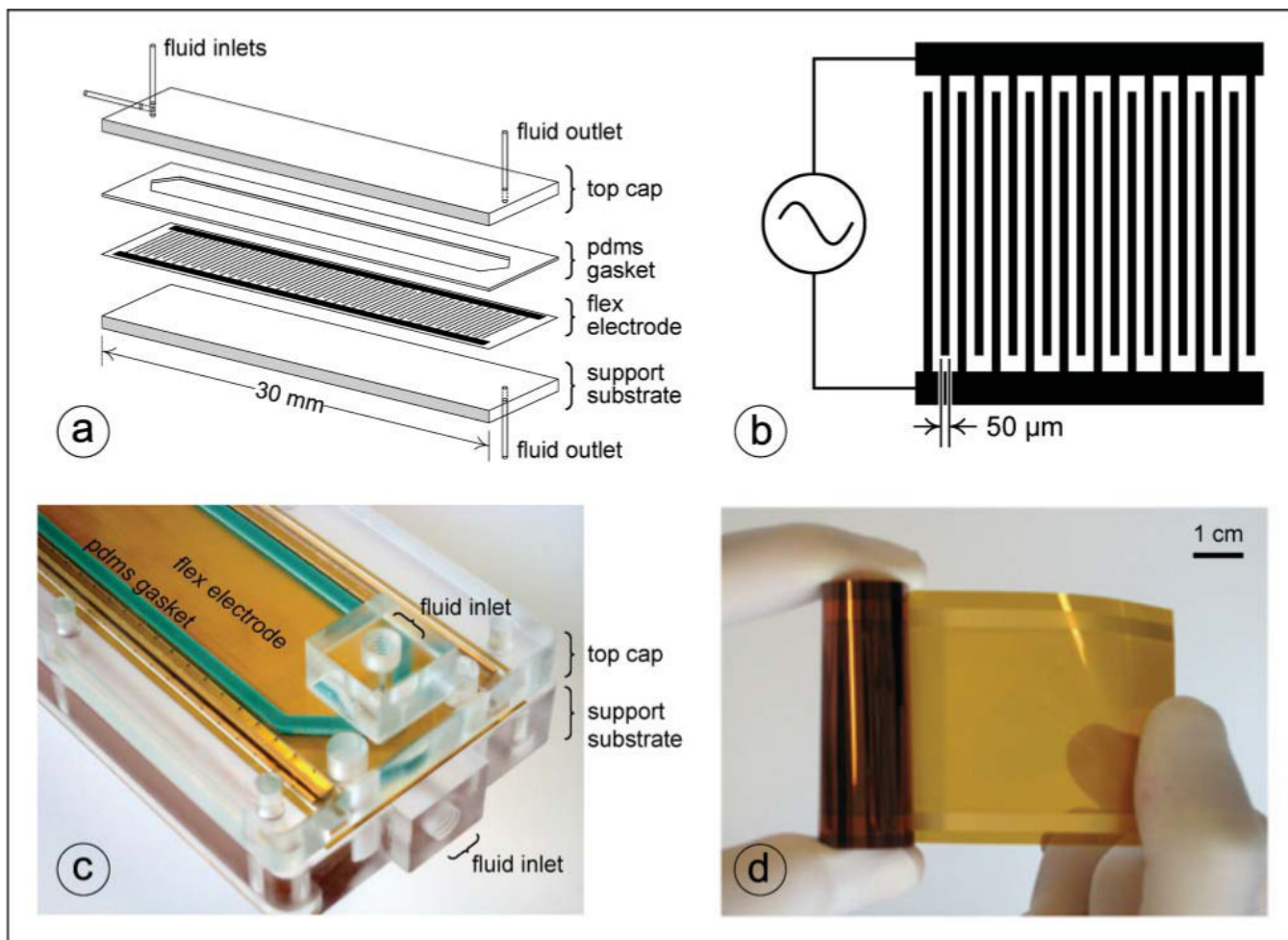


Fig. 2. DEP-FFF instrumentation. (a) Exploded diagram of DEP-FFF separator chamber showing support and top substrates, flex electrode, PDMS gasket, and fluid ports. (b) Schematic of interdigitated electrode array (not to scale). (c) Close-up of inlet portion of assembled stacked-polymer DEP-FFF separator chamber showing support and top substrates, flex electrode, PDMS gasket, and fluid ports. (d) Continuous flex-circuit reel of 50 μm -wide gold microelectrodes on polyimide substrate.

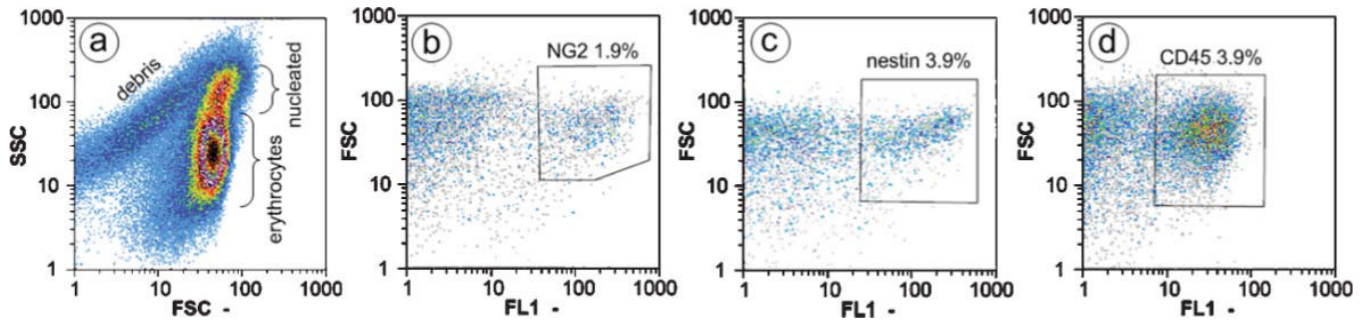


Fig. 3.

Immunolabeling and flow cytometric analysis of adipose-derived cell mixture. (a) Ungated cytogram of starting SVF cell mixture showing the relative abundance of cellular debris, erythrocytes and leukocytes/nucleated cells. (b–d) Fluorescence (FL1) of immunolabeled cell samples was analyzed to determine the percentage of (b) NG2-positive cells (1.9%), (c) nestin-positive cells (3.9%) and (d) CD45-positive cells (3.9%) relative to total cell number (gated to exclude submicron debris). Isotype controls were performed (data not shown).

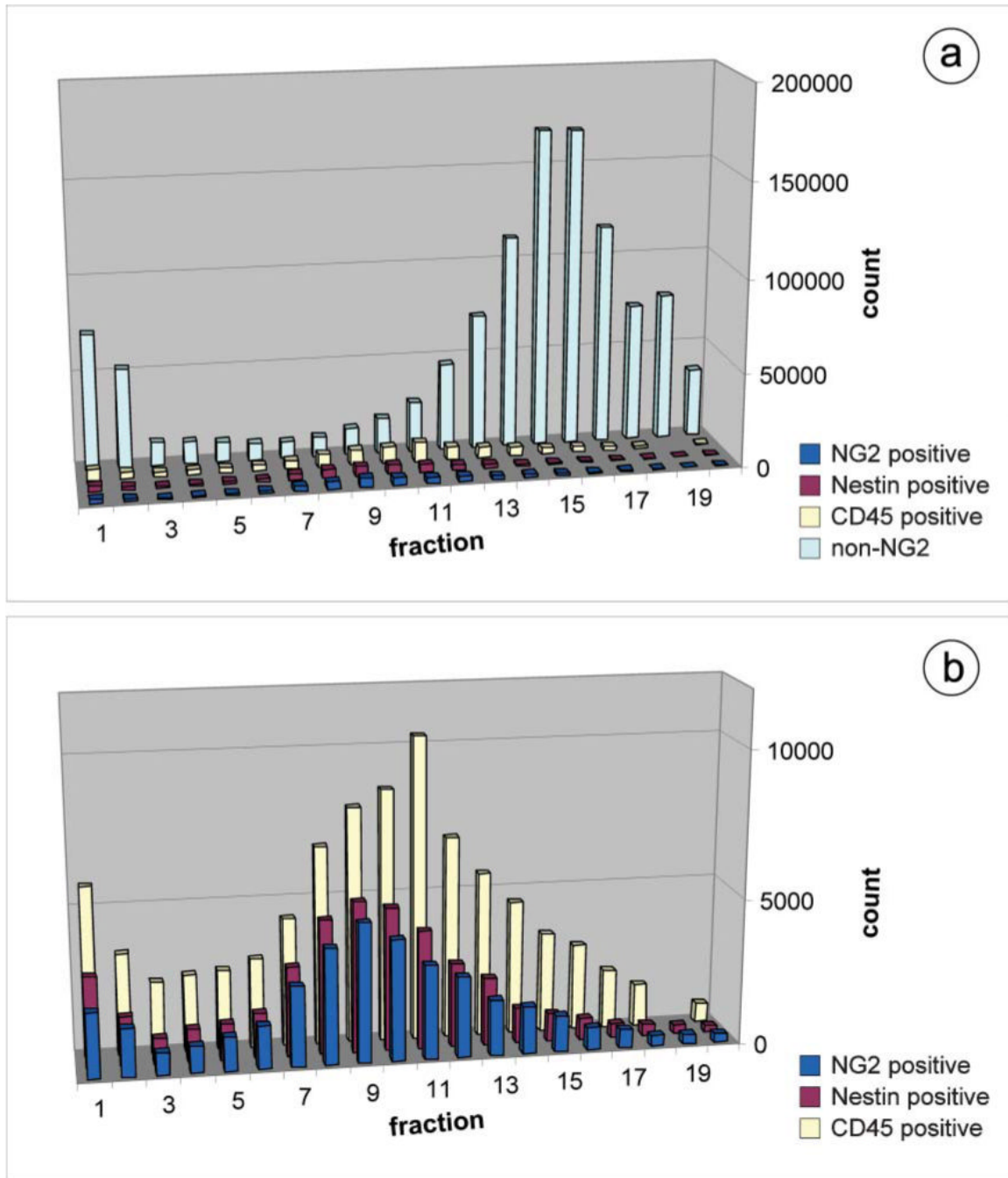


Fig. 4. DEP-FFF fractionation of adipose-derived cell mixtures. (a) Overlay of separate DEP-FFF elution profiles for adipose-derived cell mixtures from a representative patient sample immunolabeled to detect NG2 (blue), nestin (maroon), or CD45 (yellow); NG2-negative particles from the NG2 run are shown in light blue. (b) Detail of elution profile overlays for adipose-derived cell mixtures immunolabeled to detect NG2 (blue), nestin (maroon), or CD45 (yellow).

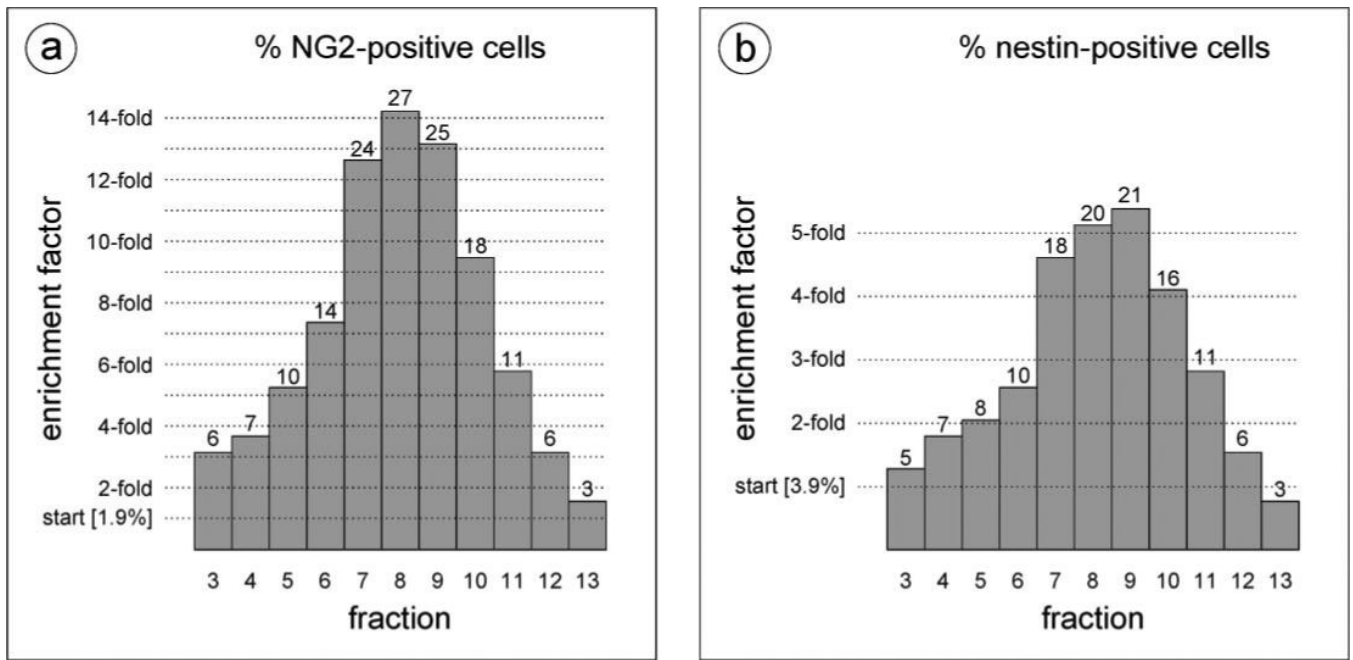


Fig. 5. Relative enrichment of cells positive for (a) NG2 or (b) nestin after DEP-FFF processing.